

# Ion-induced atomic excitation in Vanadium

A. Bachrak<sup>a</sup>, L. Jadoual<sup>b</sup>, K. Bria<sup>a</sup>, and M. Ait El Fqih<sup>a,\*</sup>

<sup>a</sup>Laboratory of Artificial Intelligence & Complex Systems Engineering,  
National Graduate School of Arts and Crafts, Hassan II University, Casablanca, Morocco.

<sup>b</sup>Laboratoire “LAMIGEP” Ecole Marocaine des Sciences de l’Ingénieur EMSI–Marrakech-Maroc.

\*e-mail: m.aitelfqih@gmail.com

Received 10 July 2024; accepted 12 December 2024

Light emission from pure vanadium in the presence and absence of oxygen under 5 keV Kr<sup>+</sup> ions bombardment is studied. Neutral V I (318.3 nm) spectral line shows a transient at beam-off conditions. The transient curve follows the characteristic of an oxide sputtering. Sputtering yields of adsorbed oxygen on V are calculated using SRIM and SDTrimSP from the spectral line V I 318.3 nm with the assumptions that a monolayer of oxygen is adsorbed on vanadium with its surface exposed to the oxygen flux and that negligible recoil implantation of oxygen in vanadium is taking place. The tendency of sputtering yields (as a function of beam fluence) is supposed to be due to the overlapping of individual collision cascades generated in the interaction of various components of Kr<sup>+</sup> projectile with the vanadium surface.

**Keywords:** Sputtering; Transient effect; Vanadium; SRIM; SDTrimSP.

DOI: <https://doi.org/10.31349/RevMexFis.71.031003>

## 1. Introduction

Ion beam sputtering is a valuable technique employed for surface analysis and exploration of materials for analytical purposes. Among the various methods available, Secondary Ion Mass Spectrometry (SIMS) stands out as the most sensitive technique. SIMS identifies ejected particles by their mass, providing high precision and sensitivity in surface analysis. In contrast, emission of optical spectra [1, 6], which utilizes the emitted light, offers distinct benefits in surface analysis. One key advantage of optical spectroscopy lies in its unambiguous identification of elements through a set of atomic lines. Furthermore, when dealing with insulating targets [7], optical spectroscopy is less susceptible to interference from space charge issues, making it an attractive choice. Additionally, this technique is cost-effective and relatively user-friendly. However, it is essential to address the challenges posed by the alteration of the material’s surface during ion beam bombardment, especially when employing high ion currents to enhance sensitivity. The alterations induced by ion bombardment encompass both geometric and chemical transformations. Geometrically, the bombardment process can lead to the growth of microreliefs on the sample’s surface, particularly evident in polycrystalline materials [9]. The primary objective of this paper is to assess and discuss the ramifications of these surface alterations when utilizing ion beam optical spectroscopy for the analysis of pure vanadium and air-oxidized vanadium samples. By comprehensively evaluating these effects, we aim to provide insights into the practical implications of employing this technique in surface analysis.

## 2. Experimental

The experimental setup used in this study has been previously detailed in references [11]. It involves the generation of a

5 keV Kr<sup>+</sup> ion beam with a typical intensity of 2  $\mu$ A and a cross-sectional area of 1 mm<sup>2</sup> at an incident angle of 70 degrees. Light is detected at a right angle from the ion beam in the plane of incidence. The detector is a photomultiplier, so the time evolution is obtained either by following the intensity of a given atomic line or by carrying out partial or complete scans from time to time. The samples are prepared by mechanical polishing and ultrasonic cleaning in ethanol and then placed in a high vacuum (better than 10<sup>-7</sup> torr). Pure oxygen (99.995% purity) at a pressure of 10<sup>-6</sup> torr was introduced in front of the clean vanadium target. The oxygen used is the molecular one and the gas pressure was measured by means of a Penning gauge. Prior to the start of each measurement, the vanadium target is cleaned in situ by ion beam sputtering. The ion beam current was measured directly on the sample or by a Faraday cup placed behind the target, in the direction of the ion beam. The sample holder can rotate to change the angle of incidence between the ion beam and the normal to the sample surface and translate for consecutive analysis of several samples. The spectrograph employed for this study covers a wave-length range from 190 to 590 nm. Note that the angle of incidence and the energy of the ion beam are initial conditions.

### 2.1. Code SRIM

The simulation was conducted using the extensively validated SRIM (Stopping Range of Ions in Matter) code which involved subjecting a significant number of incident ions to the target material [12]. In the SRIM program, the model assumes that atom-atom collisions can be reasonably approximated as elastic binary collisions, which are described by an interaction potential. Additionally, the program treats the energy loss to electrons as a separate and inelastic energy loss process. This model includes the typical model described by

the Lindhard-Scharff-Schiott (LSS) or the Ziegler-Biersack-Littmark (ZBL) model. Both models are essential for accurately predicting the energy loss of ions as they penetrate materials. To successfully run the SRIM simulation, several essential inputs were required. Some of these inputs, such as the incidence angle and the ions energy, were obtained from experimental measurements. The raw data generated by the SRIM Code are subsequently subjected to further processing using another program known as ANGULAIRE to determine the total number of ejected particles. The stopping power,  $dE/dx$ , represents the energy loss per unit path length  $dx$  of an ion as it travels through a material. It can be calculated using the Bethe-Bloch equation:

$$\frac{dE}{dx} = K \cdot \frac{Z_1^2 Z_2^2}{A} \cdot \frac{1}{\beta^2} \times \left( \ln \left[ \frac{2m_e \beta^2 c^2}{I} \right] - \beta^2 - \frac{\delta(\beta\gamma)}{2} \right), \quad (1)$$

where,  $Z_1$  and  $Z_2$  are the atomic numbers of the incident ion and the target atom, respectively,  $A$  is the atomic mass,  $\beta$  is the velocity of the ion relative to the speed of light,  $\gamma$  represents the Lorentz factor,  $m_e$  is the electron mass,  $I$  is the mean excitation energy of the target material, and  $K$  is a constant.

SRIM uses these formalisms to simulate the behavior of ion beams in materials, providing valuable information about ion penetration depth, energy loss, and scattering effects. The actual implementation in SRIM involves more advanced numerical techniques, Monte Carlo simulations, and databases of material properties to provide accurate results for a wide range of ion-material combinations and energies.

## 2.2. SDTrimSP code

SDTrimSP (Swift Dark Matter Trimmed Simulation Package) is a software tool used for simulating the passage of dark matter particles through a solid-state detector [13]. It is commonly used in the field of experimental particle physics to model the interactions between dark matter candidates and detector materials. The main calculations performed by SDTrimSP include Energy Loss, Trajectory and Range and Scattering Cross-Sections. SDTrimSP calculates the scattering cross-sections for different types of interactions between dark matter particles and atomic nuclei in the detector material. This is essential for predicting the likelihood of specific interaction processes occurring. SDTrimSP is a valuable tool for researchers in the field of dark matter detection, as it allows them to optimize detector designs, analyze experimental data, and make predictions about the expected dark matter signal in their experiments. The SDTrimSP is designed to simulate atomic collisions in amorphous targets. It calculates ranges, reflection coefficients and sputtering yields as well as more detailed information like depth distributions of implanted and energy distributions of backscattered and sputtered atoms. The program is based on the binary collision

approximation and uses the same physics as its predecessors TRIM.SP and TRIDYN, but the structure of the new program has been completely changed. It runs on all sequential and parallel platforms with a F90 compiler. The mathematical formalism behind the calculations performed by SDTrimSP involves various physics models and equations. Here are some of the key components of the mathematical formalism used in SDTrimSP: Stopping Power Calculation: To determine the energy loss of dark matter particles as they traverse a material, SDTrimSP typically employs the Bethe-Bloch formula or other similar equations. The Bethe-Bloch formula relates the stopping power (energy loss per unit length) to the charge and velocity of the incoming particle, as well as the properties of the target material. Formula (Simplified):

$$\frac{-dE}{dx} = -\frac{4\pi Z^2 z^2 e^4}{mv^2} \left( \ln \left[ \frac{2mv^2}{I} \right] - \beta^2 \right), \quad (2)$$

where  $e$  is the elementary charge,  $z$  is the charge of the incoming particle,  $m$  is the mass of the incoming particle,  $v$  is the velocity of the incoming particle, and  $Z$  is the atomic number.

Trajectory Calculation: The trajectory of the particle can be calculated using equations of motion, typically the equations for a charged particle moving through a medium subject to electromagnetic forces. These equations describe how the particle's position changes as a function of time. Cross-Section Calculations: To determine scattering cross-sections for different interaction processes, various quantum mechanical formalisms are used, depending on the specific interactions under consideration. Cross-sections are often calculated based on quantum scattering theory. SDTrimSP may use statistical distributions and models based on the energy loss and interaction cross-sections. The specific formalism for signal generation can vary depending on the detector type and experimental conditions. The actual mathematical details and equations used in SDTrimSP can be quite complex and depend on the specific interactions being studied, the detector material, and the particle properties. Researchers using SDTrimSP typically refer to its documentation and user guides for a more comprehensive understanding of the mathematical formalism and how to configure the software for their specific experiments.

## 3. Results

During our investigation, the increase in photon yield was observed in the wavelength range explored at 318.3 nm. The results of this observation are depicted in Fig. 1.

Remarkably, the maximum intensity was attained just 7 minutes after the initiation of ion bombardment. Subsequently, the signal experienced a rapid decline, indicating dynamic surface changes. Notably, our findings reveal that light intensity can be significantly influenced by surface contamination, particularly the presence of oxygen [14]. In a related context, a noteworthy study [15] reported a remarkable fivefold increase in light intensity emitted by vanadium

atoms when a surface covered with oxygen, was subjected to bombardment by 300 keV Ar<sup>+</sup> ions. These observations underscore the intricate interplay between surface conditions and the emitted light intensities during ion beam interactions.

The vanadium and its oxide have received tremendous research interest in recent years for its versatile electronic application possibilities based on its reversible metal-insulator transition behavior, which can be triggered by a large set of stimuli, such as current, electric field, or light [16]. One set of experiments is conducted under base pressure conditions, approximately at 10<sup>7</sup> torr, while the other involves the introduction of oxygen gas, leading to a pressure of around 10<sup>4</sup> torr. One significant aspect of our investigation involves the comparison of the experimental oxygen sputtering yield with simulations performed using the SRIM-code program. Encouragingly, our experimental results and the simulations exhibited a high degree of concordance, indicating that our model and the actual observations align closely. A parallel augmentation in photon yield has previously been documented in the case of silicon (Si) [14]. This phenomenon has been attributed to specific factors worth considering. Firstly, the presence of an oxide surface impedes electron tunneling, altering the dynamics of electron transitions. Furthermore, it is important to note that the oxide layer possesses a larger band gap compared to the corresponding pure metal. This variance in band gap energy favors radiative transitions, ultimately resulting in an amplification of the photon yield observed during these interactions. The transient behavior observed in Fig. 1 can be effectively characterized using the relationship elucidated by Bhattacharyya *et al.* in their previous work [17]:

$$I(\theta) = I_c + (I_0 - I_c) \exp\left(-\frac{\phi_i Y_0}{N_s} t\right). \quad (3)$$

In this context, we define various parameters:  $I(\theta)$  represents the photon intensity when the surface is partially covered with oxygen.  $I_0$  denotes the photon intensity when the surface is completely covered with oxygen.  $I_c$  signifies the

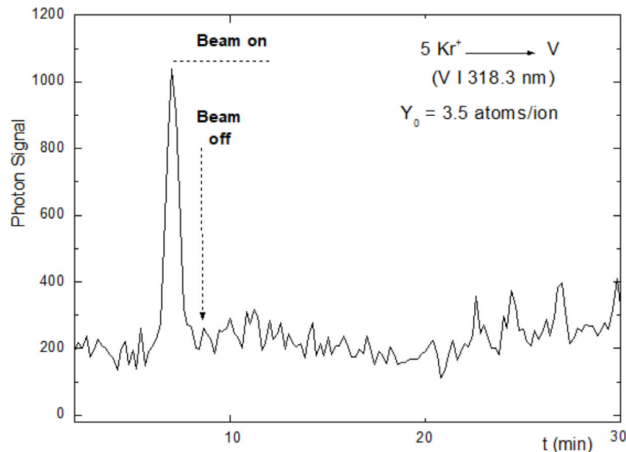


FIGURE 1. Intensity of the Neutral V I 318.3 nm during the bombardment of vanadium target by 5 KeV Kr<sup>+</sup> (For one scan).

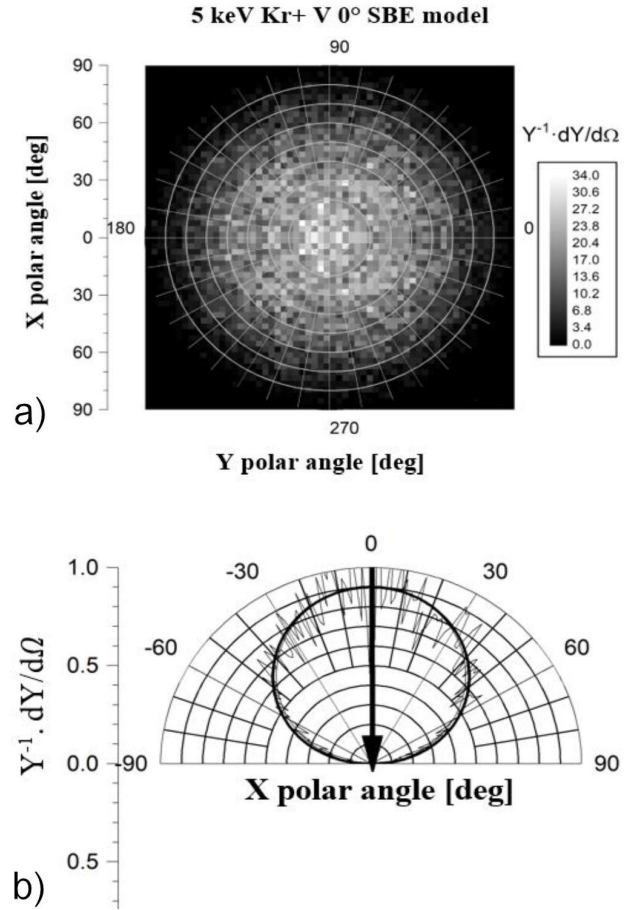


FIGURE 2. a) SDTrimSP simulation of the angular distribution of sputtered vanadium atoms for ion irradiation with 5 keV Kr<sup>+</sup> at 0°. b) Stereographic projection plot of the angular distribution of sputtered atoms for 5 keV Kr<sup>+</sup> ions at normal ion incidence on pure vanadium.

photon intensity when the surface is clean, devoid of oxygen coverage.  $\phi_i$  represents the flux density of the incident ion beam.  $N_S$  stands for the number density of adsorption sites present on a random V surface.  $Y_0$  corresponds to the best-fit value, which is directly associated with the sputtering yield of adsorbed oxygen on vanadium. These parameters collectively play a crucial role in characterizing the behavior of photon intensities during ion beam interactions with oxygen-covered vanadium surfaces. Table I presents a comprehensive overview of the theoretical sputtering yields for a vanadium target, calculated using both SRIM and SDTrimSP methodologies (Figs. 2 and 3). In Fig. 2, two key representations are provided to elucidate the behavior of sputtered vanadium atoms under specific experimental conditions. Figure 2a) presents the results of a simulation using the SDTrimSP model. This simulation focuses on the angular distribution of vanadium atoms that are sputtered when subjected to ion irradiation with 5 keV Kr<sup>+</sup> at an incidence angle of 0°. This simulation provides valuable insights into the directional pattern of sputtered vanadium atoms under the specified ion

TABLE I. Sputtering yield of vanadium.

Ion	Sputtering yields (atoms/ion)		
	SRIM-code (V-V)	SDTrimSP-code (V-V)	Transients (V-O)
Kr	4.2	5.3	3.9

irradiation conditions. Figure 2b) displays a stereographic projection plot. This plot is designed to offer a visual representation of the angular distribution of sputtered atoms. Specifically, it illustrates how vanadium atoms are distributed in terms of direction when exposed to 5 keV  $\text{Kr}^+$  ions at normal ion incidence on pure vanadium. The stereographic projection provides a comprehensive view of the spatial distribution of sputtered atoms, aiding in the analysis and interpretation of the experimental results. Together, these representations contribute to a better understanding of the behavior of sputtered vanadium atoms under the specified experimental conditions, offering valuable insights for researchers studying the interaction between ions and vanadium surfaces.

Figure 3 offers a comprehensive examination of the simulated angular distribution of sputter-ejected vanadium  $V$  particles using the SRIM model. The figure focuses on the angular dispersion of these particles, showcasing their directional spread concerning the normal of the vanadium target surface. Utilizing SRIM, a prominent tool for simulating ion-material interactions, the analysis provides crucial insights into the stopping range and angular behavior of sputtered particles. In our study,  $Y_0 = 3.5$  atoms/ion. Specifically, the simulation concentrates on vanadium particles ejected from the target during the sputtering process. This visual representation aids researchers in understanding the scattering dynamics of sputtered particles and serves as a valuable resource for those investigating sputtering processes and the intricacies of particle behavior during ion interactions with vanadium targets. In the theoretical estimates of sputtering yields for vanadium's clean surface, the calculations account for ion interactions as well as the

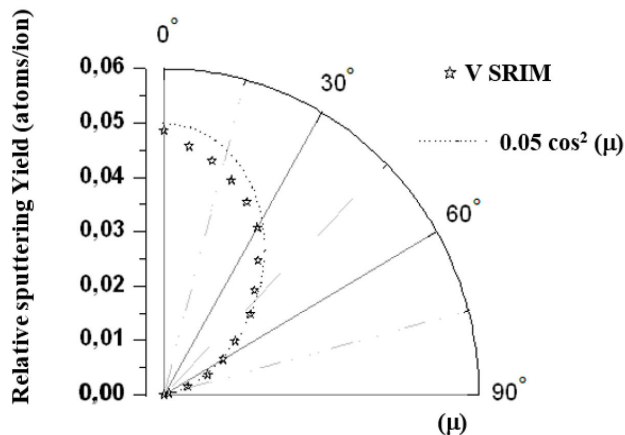


FIGURE 3. Simulated angular distribution (SRIM) of sputter-ejected  $V$  particles from the vanadium target.

intricate V-V interactions occurring within the collision cascades. In stark contrast, the sputtering yields extracted from the transient data stem from a more complex interplay of interactions, involving V-O and ion-O interactions within the collision cascades. This subtle yet crucial difference underscores the multifaceted nature of sputtering processes and highlights the importance of considering various factors in the analysis of such phenomena.

## 4. Discussion

The potential for achieving accurate quantitative analysis hinges on precise calibration techniques. At the onset of bombardment, a substantial portion of surface contaminants is removed rapidly, resulting in a pronounced transient signal. This initial phase is critical for defining baseline conditions, as the presence of reactive species significantly influences the signal until a layer approximately  $1 \mu\text{m}$  thick is eroded. While this behavior provides an easily recognizable signature for calibration purposes, it introduces a limitation for submicron-level analysis. This limitation stems from the overlap between the transient signal and the underlying material's true response, requiring sophisticated techniques to decouple these effects. Possible strategies include optimizing the sputtering parameters, applying in situ corrections, or using time-resolved measurements to isolate the transient contributions. For intrinsically inhomogeneous target materials, interpreting the results becomes even more challenging. Variations in material composition and structure, combined with potential surface modifications during sample preparation, exacerbate the complexity of the analysis. Uneven erosion patterns are a common issue, leading to the formation of recesses and non-uniform sputtering rates. These factors prevent the establishment of a steady state for localized analysis, complicating the quantification of material composition. To address this, complementary techniques such as optical or electron microscopy are invaluable. For example, electron microscopy can provide high-resolution imaging of surface features, while spectroscopy-based approaches, like EDX (Energy Dispersive X-ray Spectroscopy), can offer spatially resolved compositional data. Combining these methods with depth profiling enables a more comprehensive understanding of the material's structural and chemical evolution. In long-term bombardment processes, such as those involved in extensive depth profiling, microrelief formation represents a significant challenge. This surface roughening introduces uncertainties in the precise location of the probed zone and

alters the local sputtering yields. The microrelief effect can be attributed to differential erosion rates driven by the material's anisotropy, crystallographic orientation, or phase distribution. These variations lead to shadowing effects and non-uniform removal of material, which in turn impact the reliability of compositional measurements. Additionally, the accumulation of microrelief can influence the incident ion trajectory, further complicating the analysis. To mitigate the effects of microrelief formation, a dynamic approach to experimental design is necessary. Periodic adjustment of the angle of incidence during bombardment can help redistribute the ion flux, minimizing shadowing, and ensuring more uniform erosion. Advanced techniques such as rotational sputtering or dual-beam bombardment may also prove effective in managing these effects. Furthermore, implementing computational models that account for the evolution of surface roughness during sputtering can provide predictive insights into the impact of microrelief on analytical outcomes.

Another key consideration is the interaction between the analyzed material and the bombardment environment. Reactive species introduced during sputtering can chemically modify the surface, influencing both the sputtering yields

and the measured composition. Monitoring these interactions in real time, using in situ diagnostics such as secondary ion mass spectrometry (SIMS) or x-ray photoelectron spectroscopy (XPS), can enhance our ability to identify and correct for such effects.

## 5. Conclusions

The present study unveils notable variations in transient phenomena when the beam is turned off, particularly under the influence of oxygen pressure and other reactive gases. It presents a series of lines with the most intense one located at 318,3 nm and all of them attributed to V I. Broadly, at the baseline pressure, we observed a correlation between the intensity of the spectral line and the development of the adsorbed layer of reactive gas on the surface subjected to ion beam sputtering. Importantly, our experimental measurement of the oxygen sputtering yield closely matched both results obtained from experiments and simulations, indicating a reasonable agreement between theoretical predictions and observed outcomes.

1. C. W. White, Ion induced optical emission for surface and depth profile analysis, *Nucl. Instrum. Meth.* **149** (1978) 497, [https://doi.org/10.1016/0029-554X\(78\)90916-3](https://doi.org/10.1016/0029-554X(78)90916-3).
2. G. E. Thomas, Bombardment-induced light emission, *Surface Sci.* **90** (1979) 381, [https://doi.org/10.1016/0039-6028\(79\)90351-0](https://doi.org/10.1016/0039-6028(79)90351-0).
3. E. W. Thomas, Ion bombardment induced photon and Auger emission for surface analysis, *Vacuum* **34** (1984) 1031, [https://doi.org/10.1016/0042-207X\(84\)90221-5](https://doi.org/10.1016/0042-207X(84)90221-5).
4. G. Betz, Electronic excitation in sputtered atoms and the oxygen effect, *Nucl. Instrum. Meth. B* **27** (1987) 104, [https://doi.org/10.1016/0168-583X\(87\)90011-5](https://doi.org/10.1016/0168-583X(87)90011-5).
5. V. Kharchenko, M. Chassé and W. Szymczak, Sputtered atoms, in: *Sputtering by Particle Bombardment III*, Eds. R. Behrisch, K. Wittmaack, *Topics Appl. Phys.* **64** (1991) 91.
6. M. Ait El Fqih, and P.-G. Fournier, Ion beam sputtering monitored by optical spectroscopy, *Acta Physica Polonica A* **115** (2009) 901, <https://doi.org/10.12693/APhysPolA.115.901>.
7. M. Ait El Fqih, and P.-G. Fournier, Optical emission from Be, Cu and CuBe targets during ion beam sputtering, *Nucl. Instrum. Methods B* **267** (2009) 1206, <https://doi.org/10.1016/j.nimb.2009.01.159>.
8. L. Jadoual, A. Afkir, A. El Bouilardi, M. Ait El Fqih, R. Jour-dani, and A. Kaddouri, Ion-photon emission from titanium target under ion beam sputtering, *Nucl. Phys. At. Energy* **22** (2021) 358, <https://doi.org/10.15407/jnpae2021.04.358>.
9. M. Ait El Fqih, Angular distribution of sputtered alloy. Experimental and simulated study, *Eur. Phys. J. D* **56** (2010) 167, <https://doi.org/10.1140/epjd/e2009-00272-8>.
10. L. Jadoual, A. Afkir, A. El Bouilardi, M. Ait El Fqih, R. Jour-dani, and A. Kaddouri, Ion-photon emission from titanium target under ion beam sputtering, *Nucl. Phys. At. Energy* **22** (2021) 358.
11. J. Ziegler, M. Ziegler and J. Biersack, SRIM-The stopping and range of ions in matter, *Nuclear Instruments and Methods in Physics Research B* **268** (2010) 1818, <https://doi.org/10.1016/j.nimb.2010.02.091>.
12. H. Hofsässa, K. Zhang, and A. Mutzke, Simulation of ion beam sputtering with SDTrimSP, TRI-DYN and SRIM, *Appl. Surf. Sci.* **310** (2014) 134, <https://doi.org/10.1016/j.apsusc.2014.03.152>.
13. A.H. Dogar, S. Ullah, S. Hussain, and A. Qayyum, Survival of the excited Mg atoms sputtered from Mg, MgO, MgF2 and oxygen-covered Mg surface, *Appl. Surf. Sci.* **255** (2008) 3235, <https://doi.org/10.1016/j.apsusc.2008.09.024>.
14. S. Reinke, D. Rahmann, and R. Hippler, Light emission from sputtered atoms following ion bombardment of polycrystalline Al and Cu targets, *Vacuum* **42** (1991) 807, [https://doi.org/10.1016/0042-207X\(91\)90113-w](https://doi.org/10.1016/0042-207X(91)90113-w).
15. A. Varanasi, N. Devabharathi, M. Divya, S. Kumar Mondal, and S. Dasgup, Printed and Room Temperature Processed Nanoparticulate VO2 Thin Films Toward Memristive Device Applications, *IEEE Journal on Flexible Electronics* **2** (2023) 5, <https://doi.org/10.1109/JFLEX.2023.3278234>.

16. S. R. Bhattacharyya, J. F. van der Veen, C. B. Kerkdijk, and F. W. Saris, Bombardment induced light emission from silicon, silicon nitride and silicon carbide surfaces, *Rad. Eff.* **32** (1977) 25. <https://doi.org/10.1080/00337577708237452>.
17. S. R. Bhattacharyya, U. Brinkmann, and R. Hippler, Investigation of relative sputtering yields during ionoluminescence of Si, *Appl. Surf. Sci.* **150** (1999) 107. [https://doi.org/10.1016/S0169-4332\(99\)00229-9](https://doi.org/10.1016/S0169-4332(99)00229-9).